International Journal of Advanced Information Science and Technology (IJAIST) ISSN: 2319:2682
Vol.6, No.11, November 2017 DOI:10.15693/ijaist/2017.v6i11.495-499

Removal of haze from videos Using Color Attenuation Prior

Mrs.Y.Jalajakshi
Research Scholar Rayalaseema University

Abstract— Removal of haze from videos has been a challenging problem due to its ill-posed nature. In this paper,we propose a simple but powerful color attenuation prior for haze removal. By creating a linear model for modeling the scene depth of the hazy image under this novel prior and learning the parameters of the model with a supervised learning method, the depth information can be well recovered. With the depth map of the hazy image, we can easily estimate the transmission and restore the scene radiance via the atmospheric scattering model, and thus effectively remove the haze from video.

Index Terms— dehazing, image restoration, depth restoration.

1. INTRODUCTION

Images taken in bad weather usually lose contrast and fidelity, resulting from the fact that light is absorbed and scattered by the turbid medium such as particles and water droplets in the atmosphere during the process of propagation. Moreover, most automatic systems, which strongly depend on the definition of the input images, fail to work normally caused by the degraded images. Therefore, improving the technique of image haze removal will benefit many image understanding and computer vision applications such as aerial imagery [1], image classification [2]–[5], image/video retrieval [6]–[8], remote sensing [9]–[11] and video analysis and recognition [12]–[14].Since concentration of the haze is different from place to place and it is hard to detect in a hazy image, Image dehazing is thus a challenging task. Early researchers use the traditional techniques of image processing to remove the haze from a single image (for instance, histogram-based dehazing methods [15]–[17]). However, the dehazing effect is limited, because a single hazy image can hardly provide much information. Later, researchers try to improve the dehazing performance with multiple images. In [18]–[20], polarization- based methods are used for dehazing with multiple images which are taken with different degrees of polarization. In [24] and [25], dehazing is conducted based on the given depth information. In this paper, we propose a novel color attenuation prior for image dehazing. This simple and powerful prior can help to create a linear model for the scene depth of the hazy image. By learning the parameters of the linear model with a supervised learning method, the bridge between the hazy image and its corresponding depth map is built effectively. With the recovered depth information, we can easily remove the haze from a single hazy image. To describe the formation of a hazy image, the atmospheric scattering model, which is proposed b y

$$\mathbf{I}(x) = \mathbf{J}(x)t(x) + \mathbf{A}(1 - t(x)), \quad (1)$$

$$t(x) = e^{-\beta d(x)}, \quad (2)$$

where x is the position of the pixel within the image, **I** is the hazy image, **J** is the scene radiance representing the haze-free image, **A** is the atmospheric light, t is the medium transmission, β is the scattering coefficient of the atmosphere and d is the depth of scene. **I**, **J** and **A** are all three-dimensional vectors in RGB space. Since **I** is known, the goal of dehazing is to estimate **A** and t, then restore **J** according to Equation (1). It is worth noting that the depth of the scene d is the most important information. Since the scattering coefficient β can be regarded as a constant in homogeneous atmosphere condition [55], the medium transmission t can be estimated easily according to Equation (2) if the depth of the scene is given. Moreover, in the ideal case, the range of $d(x)$ is $[0, +\infty)$ as the scenery objects that appear in the image can be very far from the observer, and we have:

$$\mathbf{I}(x) = \mathbf{A}, \quad d(x) \to \infty. \quad (3)$$

Equation (3) shows that the intensity of the pixel, which makes the depth tend to infinity, can stand for the value of the atmospheric light **A**. Note that, if $d(x)$ is large enough, $t(x)$ tends to be very small according to Equation (2), and $\mathbf{I}(x)$ equals **A** approximately. Therefore, instead of calculating the atmospheric light **A** by Equation (3), we can estimate A by the following equation given a

Threshold threshold :

$$\mathbf{I}(x) = \mathbf{A},\ d(x) \geq d_{thresold}. \quad (4)$$

We also notice the fact that it is not hard to satisfy this constraint: $d(x) > d_{thresold}$. In most cases, a hazy image taken outdoor has a distant view that is kilometres away from the observer. In other words, the pixel belonging to the region with a distant view in the image should have a very large depth $d_{threshold}$. Assuming that every hazy image has a distant view, we have:

$$d(x) \geq d_{thresold},\ x \in \{x \mid \forall y : d(y) \leq d(x)\} \quad (5)$$

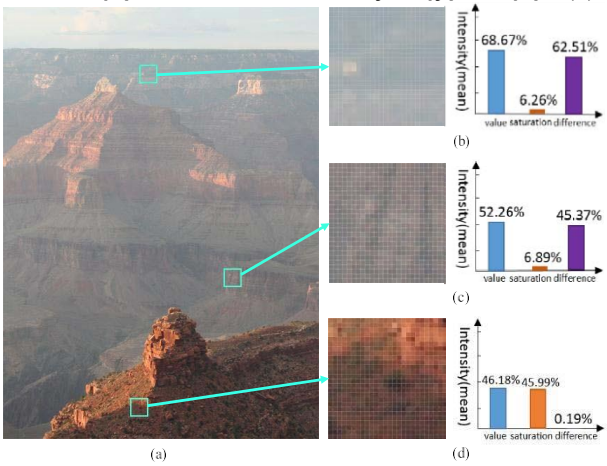

Fig. 2. The concentration of the haze is positively correlated with the difference between the brightness and the saturation. (a) A hazy image.
(b) The close-up patch of a dense-haze region and its histogram. (c) The close-up patch of a moderately hazy region and its histogram.
(d) The close-up patch of a haze-free region and its histogram

On this condition, the task of dehazing can be further con-verted into depth information restoration. However, it is also a challenging task to obtain the depth map from a single hazy image.

In the next section, we present a novel color attenuation prior which is useful for restoring the depth information from a single hazy image directly.Figure 3 illustrates the imaging process. In the haze-free condition, the scene element reflects the energy that is from the illumination source (e.g., direct sunlight, diffuse skylight and light reflected by the ground), and little energy is lost when it reaches the imaging system. The imaging system collects the incoming energy reflected from the scene element and focuses it onto the image plane. Without the influence of the haze, outdoor images are usually with vivid color (see Figure 3(a)). In hazy weather, in contrast, the situation becomes more complex (see Figure 3(b)). There are two mechanisms (the direct attenuation and the airlight) in imaging under

To understand this, we review the atmospheric scattering model. The term $\mathbf{J}(x)t(x)$ in Equation (1) is used for describing the direct attenuation. It reveals the fact that the intensity of the pixels within the image will decrease in a multiplicative manner. So it turns out that the brightness tends to decrease under the influence of the direct attenuation. On the other hand, the white or gray airlight, which is formed by the scattering of the environmental illumination, enhances the brightness and reduces the saturation. We can also explain this by the atmospheric scatter model. The rightmost term $\mathbf{A}(1-t(x))$ in Equation (1) represents the effect of the airlight. It can be deduced from this term that the effect of the white or gray airlight on the observed values is additive. Thus, caused by the airlight, the brightness is increased while the saturation is decreased. Since the airlight plays a more important role in most cases, hazy regions in the image are characterized by high brightness and low saturation.

What's more, the denser the haze is, the stronger the influence of the airlight would be. This allows us to utilize the difference between the brightness and the saturation to estimate the concentration of the haze. In Figure 4, we show that the difference increases along with the concentration of the haze in a hazy image, as we expected. Since the concentration of the haze increases along with the change of the scene depth in general, we can make an assumption that the depth of the scene is positively correlated with the concentration of the haze and we have:

Based on this assumption, the atmospheric light **A** is given by: **A** = **I**(

$$d(x) \propto c(x) \propto v(x) - s(x), \quad (7)$$

Where d is the scene depth, c is the concentration of the haze, v is the brightness of the scene and s is the saturation. We regard this statistics as color attenuation prior. Figure 5 gives the geometric description of the color attenuation prior through the HSV color model.Figure 5(a) is the HSV color model, and Figure 5(b-d) are the near, moderate-distance and far scene depths, respectively. Vector **I** indicates the hazy image, passing through the origin and performing the projec- tion of the vector **I** onto a horizontal plane Setting the angle between vector **I** and its projection as α, according to the HSV color model, when α varies between 0 and 90 degrees, the higher the value of α is, the higher the value of tangent α is, which indicates the greater the difference between the component of **I** in the direction of **V** and the component of **I** in the direction of **S**. As the depth increases, the value v increases and the saturation s ***decreases***, and therefore α *increases*. In other words, the angle α is positively correlated with the depth.

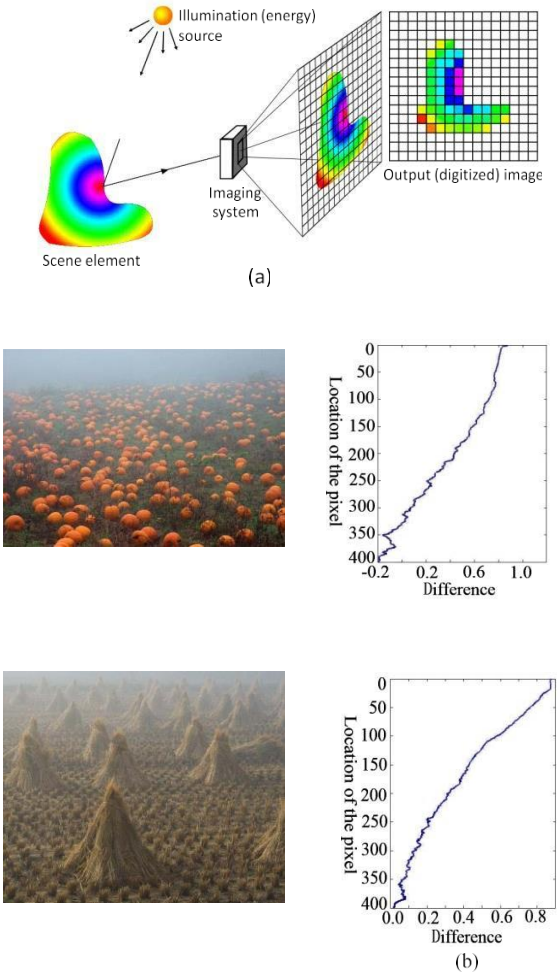

Fig. 4. Difference between brightness and saturation increases along with the concentration of the haze. (a) A hazy image. (b) Difference between brightness and saturation.

We can create a linear model, i.e., a more accurate expression, as follows:

$$d(x) = \theta_0 + \theta_1 v(x) + \theta_2 s(x) + \varepsilon(x), \quad (8)$$

where x is the position within the image, d is the scene depth, v is the brightness component of the hazy image, s is the saturation component, θ_0, θ_1, θ_2 are the unknown linear coefficients, $\varepsilon(x)$ is a random variable representing the random error of the model, and ε can be regarded as a random image. We use a Gaussian density for ε with zero mean and variable σ^2 (i.e. $\varepsilon(x) \sim N(0, \sigma^2)$). According to the property of the Gaussian distribution, we have: $d(x) \sim p(d(x)|x, \theta_0, \theta_1, \theta_2, \sigma^2) = N(\theta_0 + \theta_1 v + \theta_2 s, \sigma^2)$. (9)

One of the most important advantages of this model is that it has the edge-preserving property. To illustrate this, we Due to that σ can never be too large in practice, the value of $\varepsilon(x)$ tends to be very

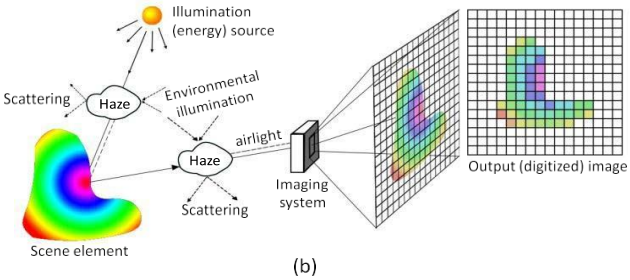

Fig. 3The process of imaging under different weather onditions. (a) The process of imaging in sunny weather. (b) The process of imaging in hazy weather.

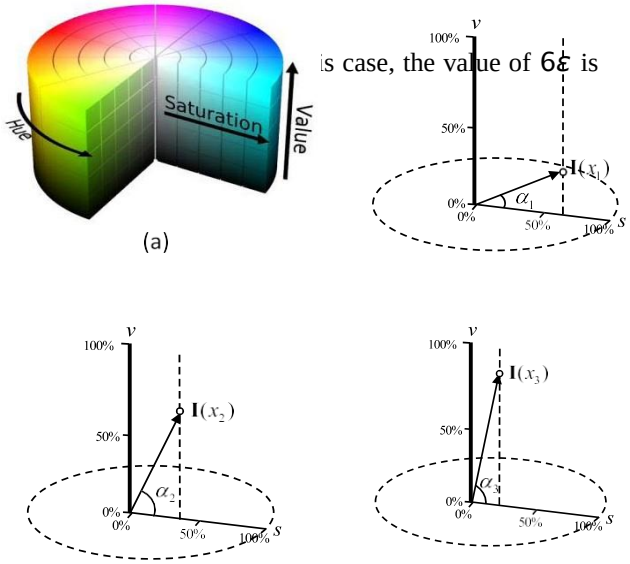

Fig. 5. The geometric description of the color attenuation prior. (a) The HSV color model. (b) The near scene depth condition. (c) The moderate-distance condition. (d) The far scene depth condition.

we have: $\nabla d = \theta_1 \nabla v + \theta_2 \nabla s + \nabla \varepsilon$. (10)

A 600×450 random image ε with $\sigma = 0.05$ and its corresponding gradient image $\delta\varepsilon$ are shown in Figure 6(e) and Figure 6(d), respectively. As can be seen, both the gradient image $\delta\varepsilon$ and the random image ε are very dark. It turns out that the edge distribution of d is independent of ε given a small σ. In addition, since v and s are actually the two single-channel images (the value channel and the saturation channel of the HSV color space) into which the hazy image **I** splits, Equation (10) ensures that d has an edge only if **I** has an edge. We give an example to illustrate this in Figure 6. Figure 6(a) is the hazy image. Figure 6(b) shows the edge distribution of the hazy image. Figure 6(c) shows the Sobel image $\delta d = \theta_1 \delta v + \theta_2 \delta s + \delta\varepsilon$, where

θ_1 is simply set to 1.0, θ_2 is set to -1.0, and ε is a random image as mentioned. As we can see, Figure 6(b) is similar.

D. Estimation of the Depth Information

As the relationship among the scene depth d, the bright- ness v and the saturation s has been established and the coefficients have been estimated, we can restore the depth map of a given input hazy image according to Equation (8). However, this model may fail to work in some particular situations. For instance, the white objects in an image are usually with high values of the brightness and low values of the saturation. Therefore, the proposed model tends to consider the scene objects with white color as being distant. Unfortunately, this misclassification will result in inaccurate estimation of the depth in some cases. Based on the assumption that the scene depth is locally constant, we process the raw depth map by:Where $K_r(x)$ is an $r \times r$ neighborhood centered at x , and d_r is the depth map with scale r . As shown in Figure 8(c), the new depth map d_{15} can well handle the geese regions. is also obvious that the blocking artifacts appear in the image. To refine the depth map, we use the guided image filtering [43] to smooth the image.In order to check the validity of the assumption, we collected a large database of outdoor hazy images from several well-known photo websites and computed the scene depth map of each hazy image with its brightness and saturation components

2. SCENE RADIANCE RECOVERY

A. Estimation of the Atmospheric Light

We have explained the main idea of estimating the atmospheric light in Section II. In this section, we describe the method in more detail. As the depth map of the input hazy image has been recovered, the distribution of the scene depth is known. Figure 10(a) shows the estimated depth map of a hazy image. Bright regions in the map stand for distant places. According to Equation (6), we pick the top 0.1 percent brightest pixels in the depth map, and select the pixel with highest intensity in the corresponding hazy image **I** among these brightest pixels as the atmospheric light **A** (see Figure 10(b) and Figure 10(c)).

B. Scene Radiance Recovery

Now that the depth of the scene d and the atmospheric light **A** are known, we can estimate the medium transmission t easily according to Equation (2) and recover the scene

Complexity

Given an image of size $m \times n$ and radius r , the complexity of the proposed dehazing algorithm is only $O(m \times n \times r)$, when the linear coefficients θ_0, θ_1, θ_2 in Equation (8) are obtained.

Ihis approach is much faster than others and achieves efficient processing even when the given hazy image is large. The high efficiency of the proposed approach mainly benefits from the fact that the linear model based on the color attenuation prior significantly simplifies the estimation of the scene depth and the transmission.

3. DISCUSSIONS AND CONCLUSION

In this paper, we have proposed a novel linear color attenu- ation prior, based on the difference between the brightness and the saturation of the pixels within the hazy image. By creating a linear model for the scene depth of the hazy image with this simple but powerful prior and learning the parameters of the model using a supervised learning method, the depth information can be well recovered. By means of the depth map obtained by the proposed method, the scene radi- ance of the hazy image can be recovered easily. Experimental results show that the proposed approach achieves dramatically high efficiency and outstanding dehazing effects as well.

Although we have found a way to model the scene depth with the brightness and the saturation of the hazy image, there is still a common problem to be solved. That is, the scattering coefficient β in the atmospheric scattering model cannot be regarded as a constant in inhomogeneous atmosphere conditions [55.To overcome this challenge, some more advanced physical models [63] can be taken into account. We leave this problem for our future work.

REFERENCES

[1] G. A. Woodell, D. J. Jobson, Z.-U. Rahman, and G. Hines, "Advanced image processing of aerial imagery," *Proc. SPIE*, vol. 6246, p. 62460E, May 2006.

[2] L. Shao, L. Liu, and X. Li, "Feature learning for image classification via multiobjective genetic programming," *IEEE Trans. Neural Netw. Learn. Syst.*, vol. 25, no. 7, pp. 1359–1371, Jul. 2014.

[3] F. Zhu and L. Shao, "Weakly-supervised cross-domain dictionary learn- ing for visual recognition," *Int. J. Comput. Vis.*, vol. 109, nos. 1–2, pp. 42–59, Aug. 2014.

[4] Y. Luo, T. Liu, D. Tao, and C. Xu, "Decomposition-based transfer distance metric learning for image classification," *IEEE Trans. Image Process.*, vol. 23, no. 9, pp. 3789–3801, Sep. 2014.

[5] D. Tao, X. Li, X. Wu, and S. J. Maybank, "Geometric mean for subspace selection," *IEEE Trans. Pattern Anal. Mach. Intell.*, vol. 31, no. 2, pp. 260–274, Feb. 2009.

[6] J. Han *et al.*, "Representing and retrieving video shots in human-centric brain imaging space," *IEEE Trans. Image Process.*, vol. 22, no. 7, pp. 2723–2736, Jul. 2013.

[7] J. Han, K. Ngan, M. Li, and H.-J. Zhang, "A memory learning frame- work for effective image retrieval," *IEEE Trans. Image Process.*, vol. 14, no. 4, pp. 511–524, Apr. 2005.

[8] D. Tao, X. Tang, X. Li, and X. Wu, "Asymmetric bagging and random subspace for support vector machines-based relevance feedback in image retrieval," *IEEE Trans. Pattern Anal. Mach. Intell.*, vol. 28, no. 7, pp. 1088–1099, Jul. 2006.

[9] J. Han, D. Zhang, G. Cheng, L. Guo, and J. Ren, "Object detection in optical remote sensing images based on weakly supervised learning and high-level feature learning," *IEEE Trans. Geosci. Remote Sens.*, vol. 53, no. 6, pp. 3325–3337, Jun. 2015.

[10] G. Cheng *et al.*, "Object detection in remote sensing imagery using a discriminatively trained mixture model," *ISPRS J. Photogramm. Remote Sens.*, vol. 85, pp. 32–43, Nov. 2013.

[11] J. Han *et al.*, "Efficient, simultaneous detection of multi-class geospatial targets based on visual saliency modeling and discriminative learning of sparse coding," *ISPRS J. Photogramm. Remote Sens.*, vol. 89, pp. 37–48, Mar. 2014.

[12] L. Liu and L. Shao, "Learning discriminative representations from RGB-D video data," in *Proc. Int. Joint Conf. Artif. Intell.*, Beijing, China, 2013, pp. 1493–1500.

[13] D. Tao, X. Li, X. Wu, and S. J. Maybank, "General tensor discriminant analysis and Gabor features for gait recognition," *IEEE Trans. Pattern Anal. Mach. Intell.*, vol. 29, no. 10, pp. 1700–1715, Oct. 2007.

[14] Z. Zhang and D. Tao, "Slow feature analysis for human action recognition," *IEEE Trans. Pattern Anal. Mach. Intell.*, vol. 34, no. 3, pp. 436–450, Mar. 2012.

[15] T. K. Kim, J. K. Paik, and B. S. Kang, "Contrast enhancement system using spatially adaptive histogram equalization with temporal filtering," *IEEE Trans. Consum. Electron.*, vol. 44, no. 1, pp. 82–87, Feb. 1998.

[16] J. A. Stark, "Adaptive image contrast enhancement using generalizations of histogram equalization," *IEEE Trans. Image Process.*, vol. 9, no. 5, pp. 889–896, May 2000.

[17] J.-Y. Kim, L.-S. Kim, and S.-H. Hwang, "An advanced contrast enhance- ment using partially overlapped sub-block histogram equalization," *IEEE Trans. Circuits Syst. Video Technol.*, vol. 11, no. 4, pp. 475–484, Apr. 2001.

[18] Y. Y. Schechner, S. G. Narasimhan, and S. K. Nayar, "Instant dehazing of images using polarization," in *Proc. IEEE Conf. Comput. Vis. Pattern Recognit. (CVPR)*, 2001, pp. I-325–I-332.

[19] S. Shwartz, E. Namer, and Y. Y. Schechner, "Blind haze separation," in *Proc. IEEE Conf. Comput. Vis. Pattern Recognit. (CVPR)*, vol. 2. 2006, pp. 1984–1991.

[20] Y. Y. Schechner, S. G. Narasimhan, and S. K. Nayar, "Polarization-based vision through haze," *Appl. Opt.*, vol. 42, no. 3, pp. 511–525, 2003.

[21] S. G. Narasimhan and S. K. Nayar, "Chromatic framework for vision in bad weather," in *Proc. IEEE Conf. Comput. Vis. Pattern Recognit. (CVPR)*, Jun. 2000, pp. 598–605.

[22] S. K. Nayar and S. G. Narasimhan, "Vision in bad weather," in *Proc. IEEE Int. Conf. Comput. Vis. (ICCV)*, vol. 2. Sep. 1999, pp. 820–827.

[23] S. G. Narasimhan and S. K. Nayar, "Contrast restoration of weather degraded images," *IEEE Trans. Pattern Anal. Mach. Intell.*, vol. 25, no. 6, pp. 713–724, Jun. 2003.

[24] S. G. Narasimhan and S. K. Nayar, "Interactive (de) weathering of an image using physical models," in *Proc. IEEE Workshop Color Photometric Methods Comput. Vis.*, vol. 6. France, 2003, p. 1.

[25] J. Kopf *et al.*, "Deep photo: Model-based photograph enhancement and viewing," *ACM Trans. Graph.*, vol. 27, no. 5, p. 116, Dec. 2008.

[26] R. T. Tan, "Visibility in bad weather from a single image," in *Proc. IEEE Conf. Comput. Vis. Pattern Recognit. (CVPR)*, Jun. 2008, pp. 1–8.

[27] R. Fattal, "Single image dehazing," *ACM Trans. Graph.*, vol. 27, no. 3, p. 72, Aug. 2008.

[28] P. S. Chavez, Jr., "An improved dark-object subtraction technique for atmospheric scattering correction of multispectral data," *Remote Sens. Environ.*, vol. 24, no. 3, pp. 459–479, Apr. 1988.

[29] K. He, J. Sun, and X. Tang, "Single image haze removal using dark channel prior," *IEEE Trans. Pattern Anal. Mach. Intell.*, vol. 33, no. 12, pp. 2341–2353, Dec. 2011.

[30] S.-C. Pei and T.-Y. Lee, "Nighttime haze removal using color transfer pre-processing and dark channel prior," in *Proc. 19th IEEE Conf. Image Process. (ICIP)*, Sep./Oct. 2012, pp. 957–960.

[31] K. B. Gibson, D. T. Vo, and T. Q. Nguyen, "An investigation of dehazing effects on image and video coding," *IEEE Trans. Image Process.*, vol. 12, no. 2, pp. 662–673, Feb. 2012.

[32] J. Yu, C. Xiao, and D. Li, "Physics-based fast single image fog removal," in *Proc. IEEE 10th Int. Conf. Signal Process. (ICSP)*, Oct. 2010, pp. 1048–1052.

[33] B. Xie, F. Guo, and Z. Cai, "Improved single image dehazing using dark channel prior and multi-scale retinex," in *Proc. Int. Conf. Intell. Syst. Design Eng. Appl.*, Oct. 2010, pp. 848–851.

[34] Q. Zhu, S. Yang, P. A. Heng, and X. Li, "An adaptive and effective single image dehazing algorithm based on dark channel prior," in *Proc. IEEE Conf. Robot. Biomimetics (ROBIO)*, Dec. 2013, pp. 1796–1800.

[35] C. Xiao and J. Gan, "Fast image dehazing using guided joint bilateral filter," *Vis. Comput.*, vol. 28, nos. 6–8, pp. 713–721, Jun. 2012.

[36] Y. Xiang, R. R. Sahay, and M. S. Kankanhalli, "Hazy image enhance- ment based on the full-saturation assumption," in *Proc. IEEE Conf. Multimedia Expo Workshops (ICMEW)*, Jul. 2013, pp. 1–4.

[37] C. Tomasi and R. Manduchi, "Bilateral filtering for gray and color images," in *Proc. 6th Int. Conf. Comput. Vis. (ICCV)*, Jan. 1998, pp. 839–846.

[38] S. Paris and F. Durand, "A fast approximation of the bilateral filter using a signal processing approach," in *Proc. Eur. Conf. Comput. Vis.*, 2006, pp. 568–580.

[39] F. Porikli, "Constant time O(1) bilateral filtering," in *Proc. IEEE Conf. Comput. Vis. Pattern Recognit. (CVPR)*, Jun. 2008, pp. 1–8.

[40] Q. Yang, K.-H. Tan, and N. Ahuja, "Real-time O(1) bilateral filtering," in *Proc. IEEE Conf. Comput. Vis. Pattern Recognit. (CVPR)*, Jun. 2009, pp. 557–564.

Author Profile

Mrs.Y.JALAJAKSHI Research Scholar Rayalaseema University. received the B.Eng. degree in Electronics and communication engineering from Andhra University, and M.Tech in Embedded Systems from JNTUH is currently a Assistant Professor with the Department of Electronics and communication. Her current research interests include, image/video processing, pattern recognition.